**Supplemental Data**

# The tarantula toxins ProTx-II and HWTX-IV differentially interact with human Nav1.7 voltage-sensors to inhibit channel activation and inactivation

Yucheng Xiao, Kenneth Blumenthal, James O. Jackson II, Songping Liang and Theodore R. Cummins

***Molecular Pharmacology***

**Supplemental Table S1.**

**Electrophysiological parameters of the voltage-dependence of steady-state activation and inactivation curves for wild type and mutant Nav1.7 channels.** Cells were held at -100 mV. Families of currents were induced by 50-ms depolarizing steps to various potential ranging from -80 to +40 mV. Recording currents from WT and mutant Nav1.7 started at 5 min after establishing whole cell configuration. The voltage dependence of steady-state inactivation was estimated using a standard double-pulse protocol, in which a 20-ms depolarizing test potential of 0 mV followed a 500-ms prepulse at potentials that ranged from -130 to -10 mV with a 10-mV increment. Data points are shown as mean ± S.E. The half-activation potential ($V_{1/2}$) and slope factor ($k$) were determined with Boltzmann fits.

| Channel | Voltage dependence of activation | | | Voltage dependence of inactivation | | |
|---|---|---|---|---|---|---|
| | $V_{1/2}$, mV | $k$, mV | $n$ | $V_{1/2}$, mV | $k$, mV | $n$ |
| hNav1.7 | -28.0 ± 0.6 | 7.7 ± 0.5 | 11 | -80.1 ± 1.0 | 7.6 ± 0.6 | 12 |
| L201V/N206D | -29.0 ± 0.5 | 7.2 ± 0.5 | 9 | -81.2 ± 0.6 | 7.4 ± 0.6 | 9 |
| F813G | -24.5 ± 0.4 | 7.7 ± 0.4 | 14 | -76.3 ± 0.6 | 7.6 ± 0.5 | 12 |
| E818C | -20.2 ± 0.3 | 7.6 ± 0.3 | 10 | -77.1 ± 0.5 | 6.4 ± 0.4 | 7 |
| E203K/E818C | -10.4 ± 0.2 | 8.9 ± 0.2 | 11 | -75.7 ± 0.5 | 6.6 ± 0.5 | 8 |
| F204A/F813G | -23.0 ± 0.6 | 7.6 ± 0.5 | 7 | -81.2 ± 0.6 | 7.4 ± 0.6 | 6 |
| F813G/E818C | -18.8 ± 0.5 | 8.3 ± 0.5 | 8 | -77.5 ± 0.6 | 7.7 ± 0.6 | 7 |
| D1586A | -26.1 ± 0.6 | 7.5 ± 0.6 | 7 | -83.1 ± 0.3 | 6.6 ± 0.2 | 7 |
| D1586E | -25.6 ± 0.4 | 6.8 ± 0.3 | 7 | -80.6 ± 0.6 | 6.9 ± 0.6 | 7 |
| E1589Q | -23.0 ± 0.4 | 7.0 ± 0.3 | 8 | -75.2 ± 0.6 | 7.0 ± 0.5 | 9 |
| T1590K | -23.9 ± 0.3 | 6.7 ± 0.3 | 9 | -77.4 ± 0.5 | 7.5 ± 0.4 | 9 |
| F1592A | -24.7 ± 0.5 | 7.3 ± 0.4 | 7 | -85.5 ± 0.4 | 6.6 ± 0.3 | 6 |
| D1586A/T1590K | -25.3 ± 0.4 | 6.8 ± 0.3 | 6 | -84.7 ± 0.4 | 7.6 ± 0.4 | 6 |
| T1590K/F1592A | -19.8 ± 0.5 | 7.9 ± 0.5 | 4 | -82.7 ± 1.0 | 8.6 ± 0.9 | 4 |

**Supplemental Table S2.**

**IC50 values for ProTx-II slowing fast-inactivation of WT sodium channel isoforms and mutant hNav1.7 channels.** $IC_{50}$ values were determined with Hill equation in Fig. 4C, Fig. 6C and Fig. 7C, in which the slope factor (*nH*) was set to 1 because only sodium channel DIV is involved in channel inactivation gating.

| Channel | $IC_{50}$, μM | Nav1.7 mutants | $IC_{50}$, μM |
|---|---|---|---|
| Nav1.2a | 4.5 ± 0.3 | D1586A | 0.05 ± 0.02 |
| Nav1.3 | 5.6 ± 0.5 | D1586E | 0.16 ± 0.02 |
| Nav1.4 | 4.2 ± 0.4 | E1589Q | 1.6 ± 0.8 |
| Nav1.5 | 4.1 ± 0.3 | T1590K | 1.4 ± 0.3 |
| Nav1.7 | 0.25 ± 0.04 | F1592A | 0.07 ± 0.01 |
| | | D1586A/T1590K | 0.26 ± 0.04 |
| | | T1590K/F1592A | 0.18 ± 0.02 |

**Supplemental Fig. S1. Sequence alignment of DIS3-S4 linker on sodium channel isoforms.** The isoforms Nav1.1, Nav1.2a, Nav1.3 and Nav1.4 are from rats while the others are from human. In (A), two conserved residues of interest are shaded in grey. In (B), two divergent residues in hNav1.7 splice variant hNav1.7a are shaded in grey. (C) Schematic showing position of mutations studied in domains I and II.

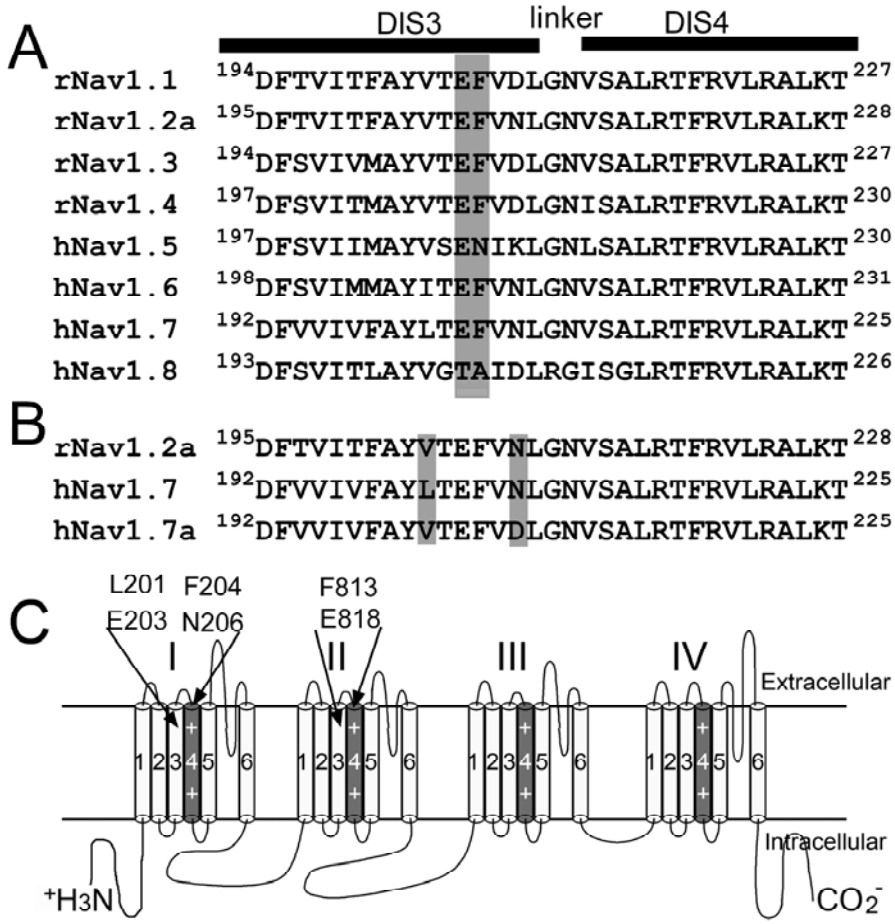

**Supplemental Fig. S2. HWTX-IV did not slow fast-inactivation of wild type (A) and mutant E818C (B) hNav1.7 channels.** Current traces were elicited by a 20-ms depolarization of -10 mV from a holding potential of -100 mV. Toxin concentrations were 1 μM for wild type hNav1.7 and 10 μM for mutant E818C hNav1.7.

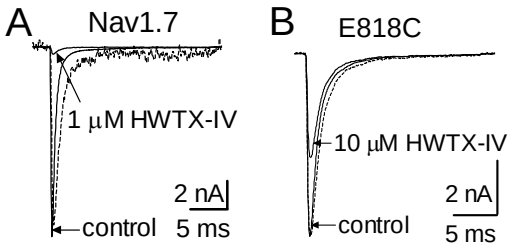

**Supplemental Fig. S3. Sequence alignment of DIIS3-S4 linkers of eight sodium channel isoforms.** The isoforms Nav1.1, Nav1.2, Nav1.3 and Nav1.4 are from rat while the others are from human. The residues that are crucial for binding to ProTx-II and HWTX-IV are shaded in grey.

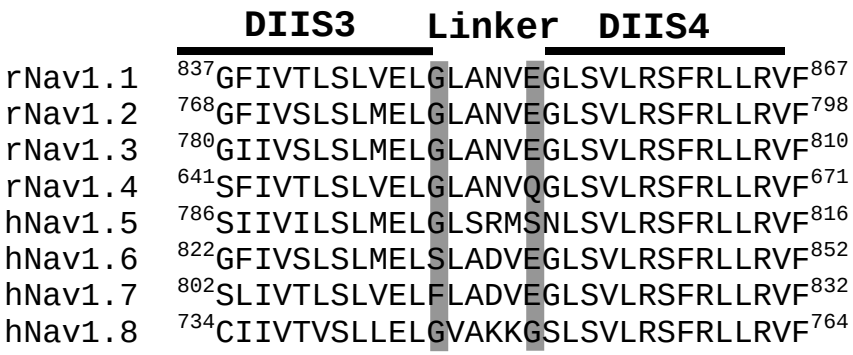

**Supplemental Fig. S4. Mutations in DIV S3-S4 linker differentially alter fast-inactivation of hNa$_v$1.7 channels expressed in HEK293 cells.** Representative current traces for five mutant (D1586A, D1586E, E1589Q, T1590K and F1592A) and WT hNa$_v$1.7 channels. The test pulse potential was -10 mV (WT hNa$_v$1.7, D1586A and D1586E) and -5 mV (E1589Q, T1590K and F1592A), respectively. Cells were held at -100 mV. The currents are shown before and after application of 0.1 or 1 μM ProTx-II, and are magnified to focus on the sustained components. Note that under control conditions hNa$_v$1.7 channels produce negligible amounts of sustained currents.

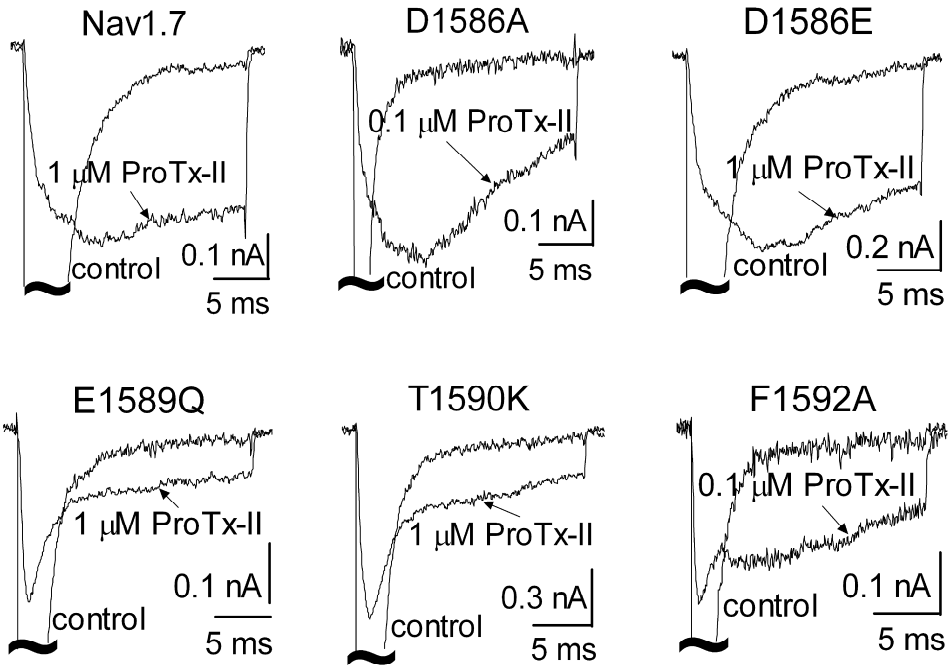

**Supplemental Fig. S5. Mutations in DIV S3-S4 linker differentially alter the effect of ProTx-II on fast-inactivation of hNa$_v$1.7-F813G/E818C double mutant channels expressed in HEK293 cells.** (A) Representative current traces for F813G/E818C, F813G/E818C/E1589Q and F813G/E818C/F1592A channels before and after exposure to ProTx-II. The test pulse potential was 0 mV. Cells were held at -100 mV. The dotted line shows the residual current in the presence of 1 μM ProTx-II after normalization to the maximum amplitude of control current. (B), Concentration-dependent inhibitory curves of ProTx-II on the activation of three mutant (F813G/E818C, F813G/E818C/E1589Q and F813G/E818C/F1592A) hNav1.7 channels. The residual current after toxin treatment was plotted as fraction of the control current. Data points (mean ± S.E., each from 3 - 6 cells) were fit with a Hill equation as described under "Experimental Procedures". Their apperant $IC_{50}$ values are 29.8, 24.6 and 26.5 nM, respectively. (C), Concentration-dependent inhibitory curves of ProTx-II on the fast-inactivation of three mutant (F813G/E818C, F813G/E818C/E1589Q and F813G/E818C/F1592A) hNav1.7 channels. The $I_{10ms}$ value was plotted as a fraction of the residual current after ProTx-II treatment. Data points (mean ± S.E., each from 3-6 cells) were fitted with Hill equation as described under "Experimental Procedure". The apparent $IC_{50}$ values are estimated to be 0.87, 4.38 and 0.11 μM, respectively.